PHOTO-ELASTIC VISUALISATION OF PHASED ARRAY ULTRASONIC PULSES IN SOLIDS

E. Ginzel[1], D. Stewart[2]
[1] Materials Research Institute - Waterloo, Ontario, Canada; [2] Oceaneering Inspection, Edmonton, Alberta, Canada

Abstract: The first images of phased-array generated ultrasonic waves in solids are demonstrated. The only previous imaging of phased array pulses have been carried out using medical probes transmitting into a liquid using schlieren optical techniques. However, schlieren techniques have proven inappropriate for industrial applications due to the inability to image the shear mode of wave propagation. This presentation uses photo-elastic imaging to illustrate the various properties of phased array probes and focal laws. Items illustrated include; wavelet formation of compression and shear modes, beam focusing and beam steering and quantitative sizing options available using image analysis of phase-formed wavefronts. It is concluded that photo-elastic visualisation is an effective tool for assessment of phased array beam forming.

Introduction: Phased array probes have been around since the 1960s in the medical industry. Visualisations have been carried out on medical arrays using schlieren techniques. Although schlieren techniques may be appropriate for medical applications where the test media are essentially watery liquids, industrial ultrasonics involves investigations of solids and often relies on the formation of shear wave-modes. Shear waves are not supported in liquids and schlieren techniques are not able to visualise shear modes in solids. To visualise both compression and shear modes present in solids requires photoelastic visualisation techniques. Figure 1 illustrates a single element pulse in water moving towards a suspended tube 9mm diameter. This was made using a laser schlieren constructed by the writers. Figure 2 illustrates a pulse image after processing to map the pressure boundaries. This pulse was captured using scheliern apparatus from the Onda Corporation. Figure 1 shows no resolution of the wavelengths involved and Figure 2 shows poor resolutions. This inability to resolve the pulse details is due to the light pulse-length. In Figure 1 the light duration was limited to 500ns and Figure 2 was limited to 70ns. This results in the pulse moving 0.7mm and 0.1mm respectively during the illumination period. This is even more critical when imaging in solids where the wave velocities are 2 to 4 times faster than in liquids. To provide better resolution requires a shorter illumination time. The authors achieved this by constructing a spark gap light source after the design by Wyatt [1]. This became a critical aspect when consideration was given to the nanosecond delays used in beam construction of phased arrays.

The photoelastic system used for this project uses a high intensity spark with a 2-nanosecond duration. Even with the acoustic velocities of glass being 2 to 4 times faster than water the system can resolve wavelengths of compression and shear modes of nominal frequencies 7 to10MHz. The photoelastic system constructed in Waterloo has been used to provide the first images of phased array generated pulses in a solid. The preferred imaging medium is silica glass as its acoustic velocities closely match that of steel or aluminium (5950m/s compression mode and 3770m/s shear mode).

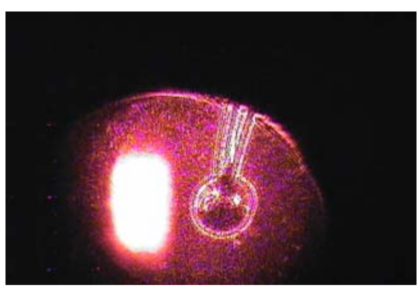

Figure 1: 500ns light pulse Schlieren

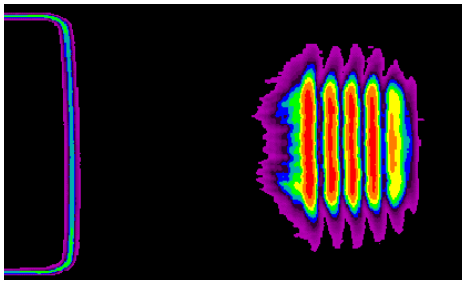

Figure 2: 70 ns light pulse Schlieren (courtesy Onda Corporation)

Results: Using an RD Tech Focus phased array instrument to drive the phased array probes, results of beam control using several focal laws are illustrated. The photoelastic technique was used to illustrate several of the common features associated with phased array systems:

1. Normal beam with varying beam width,
2. Focused normal beams,
3. Angled beams without a refracting wedge,
4. Focused angle beams without a refracting wedge
5. Angled beams with a refracting wedge,
6. Focused angle beams

Discussion: A normal beam can be made by simply pulsing several elements at the same time. The dimension of the beam is then controlled by the number of elements selected. This is illustrated in Figure 3.

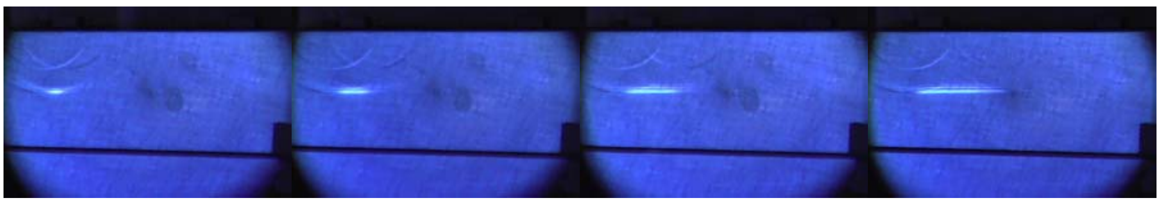

Figure 3 7.5MHz 60 element probe. Images show incremental increase of number of elements from 5 to 25 elements each starting at element number 5 in the array. Each image is taken at 15mm from the glass surface (probe immediately above).

A focused normal beam is constructed by symmetrically increasing delay to the central elements pulsed. Near zone and spot size calculations used for single elements are equally applicable to phased array focal laws.
Note how the shear mode follows the compression mode in both the unfocused and focused condition but this is more noticeable with the focused condition. This is illustrated in Figure 4.

Focusing angled shear beams is easily accomplished using the same techniques as used without a wedge. Spot size when using 8 elements can be significantly reduced when 32 elements are used to focus the beam at the same spot.

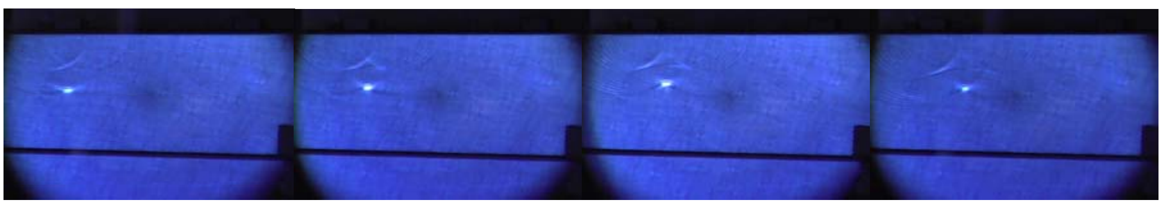

Figure 4 7.5MHz 60 element probe. Images show incremental increase of number of elements from 5 to 25 elements each starting at element number 5 in the array. Image is taken at 15mm from the glass surface.

An angled beam can be generated using a constant delay difference between adjacent elements. By altering the symmetry of delay to the elements the beam can be both angled and focused. The resultant plane or focused compression wave can also generate a shear-mode by mode conversion. Figure 5 illustrates the formation of a focused shear mode at 45° and simply entering a –45° swings the beam around to the opposite direction.

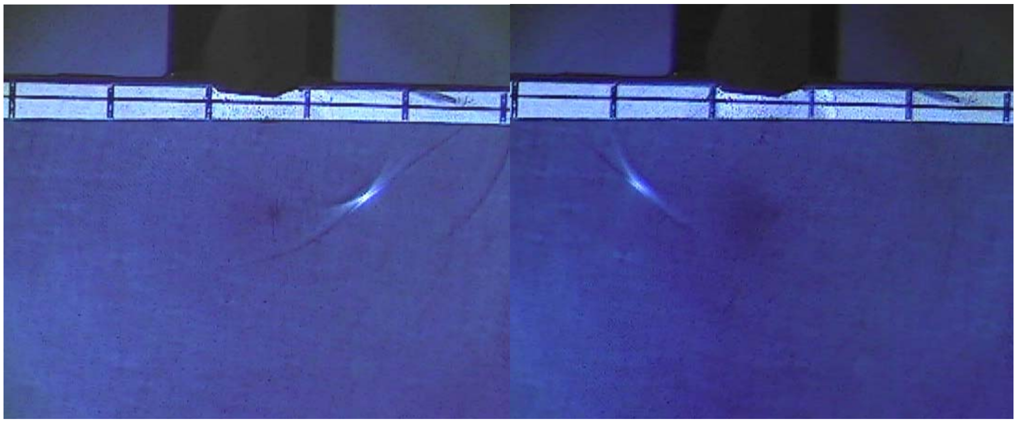

Figure 5 10MHz 32 element probe. Images show a beam both focused and angled. On the left the beam is focused at 25mm sound path and angled at 45° for the shear mode while on the right the beam is focused at 25mm and angled at –45° in shear mode. Markers on an acetate overlay indicate 1cm intervals.

Figure 6 shows the bi-modal components of a plane wave made using 12 elements in a 25 mm aperture (every other element was deactivated to better illustrate the "wavelet" composition of the wave fronts). The Angle calculated was 40° for the compression mode which results in a 24° shear mode following it.

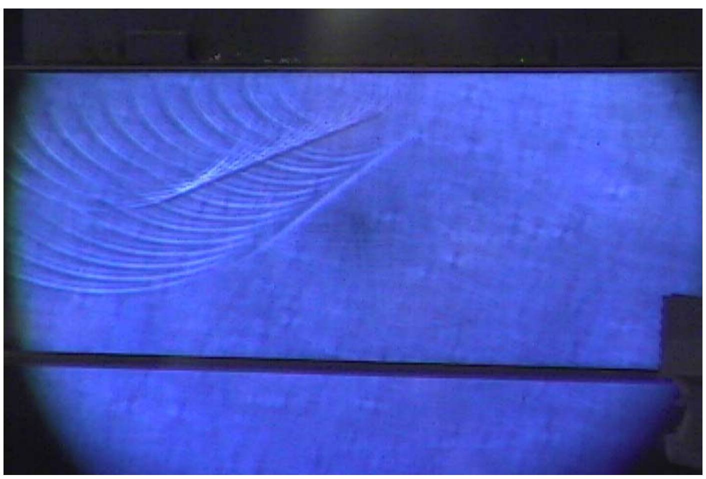

Figure 6 7.5MHz 60 element probe. Plane wavefront constructed with 12 elements with a 2mm pitch between active elements (no refracting wedge).

When the elements are mounted on a refracting wedge the degree of steering can be assisted. As well, it then becomes possible to introduce just a shear mode into the test piece. Figure 7 illustrates the pulse intensity variation that results from using 8 elements (left side) versus 16 elements (right side) in a 16mm aperture. The image on the left of Figure 7 is similar to the image in Figure 6 in that every other element was deactivated resulting in a less intense wavefront.

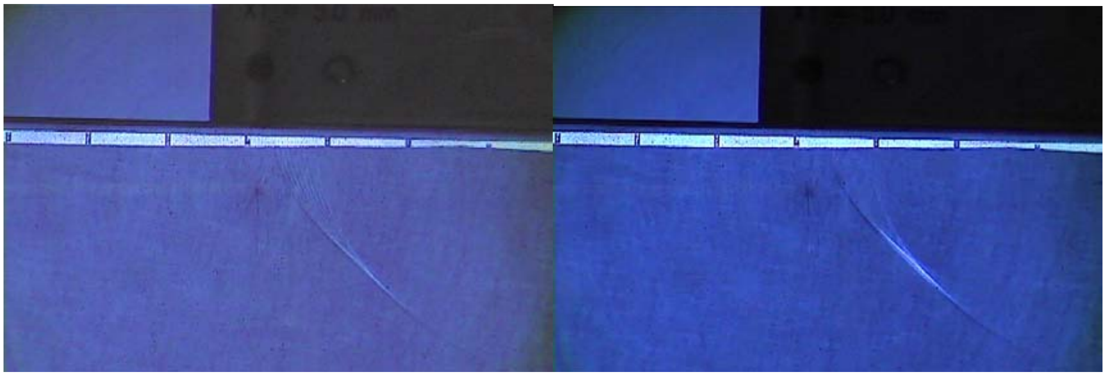

Figure 7 Image on the left is a 45 refracted plane wavefront (unfocused) using 8 elements and an "aperture" of 16mm. On the right the same plane wavefront is made using 16 elements (7.5MHz 60 element probe).

Electronic scanning allows the beam to be moved forward and backward without mechanical motion of the wedge. The effect of this is illustrated in Figure 8.

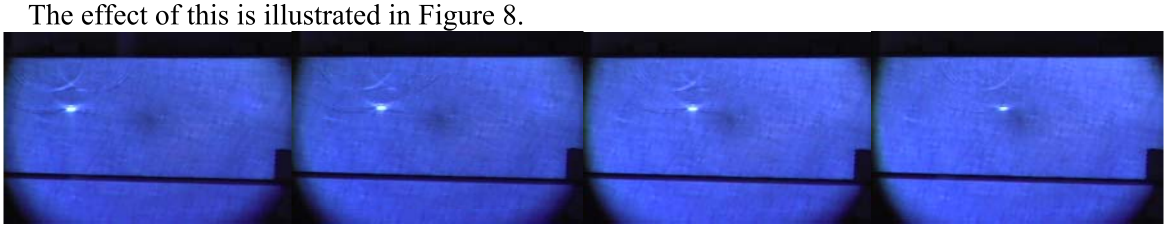

Images indicate a focused normal beam with the compression mode focused at 15mm in glass and imaged at the focal point. 12 elements are used in the focal laws of a 7.5MHz 60-element probe. The image on the left uses element number 5 as the start element of the 12 and each image then steps the focal law 5 elements further. Images indicate elements 5-16, 10-21, 15-26 and 20-31

A similar stepping of focal laws can be made by sweeping through several angles sequentially. This forms a sectorial scan or "Azimuthal" scan.

Using scaled images and a customised intensity mapping algorithm, some quantification of beam size is possible with the photoelastic images.

Figure 9 Raw image of a pulse from a 31 element focal law at 50° focused at 25mm. (7.5MHz 60-element probe with a 33° refracting wedge.

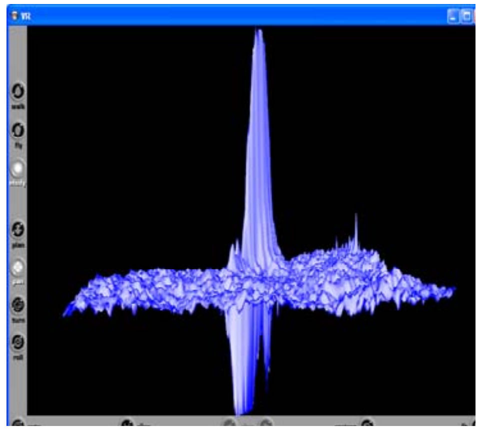

Figure 10 Processed and rendered image of the raw photo image in Figure 9.

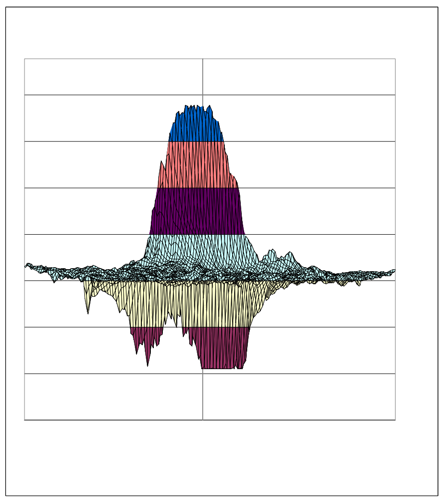

Figure 11 Spreadsheet graph of processed raw data to calculate dB drop boundaries.

Figure 9 illustrates the raw photo image (approx 14mmx14mm) of a phased array generated pulse made using 31 elements and a focal law that provided a nominal 50° refracted angle. The image was capture near the intended focal spot. Figure10 indicates the notable bi-polar nature of the pulse upon digital photo processing.
Figure 12 indicates a scaled pressure plot allowing determination of the 6dB drop that would be traditionally determined using a side drilled hole and probe displacements and corrections for angle. Using the positive phase drop to 71° of maximum (equiv. to -6dB in pulse-echo) indicates a beam dimension of 0.78mm. The calculated ideal size is about 0.6mm

Conclusions: Phased array probes are made with a variety of element sizes, numbers and frequencies. Optimising the probes for specific geometries or steering capabilities can be modelled and then confirmed using photo-elastic visualisation. As well, detection of faulty elements or problems with focal laws or pulser electronics can be checked using photoelastic visualisations. Visualisation permits a quantification of beam dimensions that is independent of target interactions.

Acknowledgements: The authors would like to thank RD Tech (especially Gaetan Fortier) for providing the ultrasonic phased array hardware used in this project. Also, thanks are extended to Oceaneering Inspection for their cooperation in the efforts to gather the data used in the assembly of the video version of this work.

References:
1. R.C. Wyatt, Imaging Ultrasonic Beams in Solids, British Journal of NDT, vol. 17, page 133, Sept. 1975